

Hysteresis and the onset of fast magnetic reconnection

P. A. Cassak, M. A. Shay, and J. F. Drake
University of Maryland, College Park, MD 20742

(Dated: December 2, 2024)

The transition between resistive (slow) and Hall-mediated (fast) magnetic reconnection with varying resistivity is elucidated using basic theoretical arguments and supported by two-fluid numerical simulations. We show that, for intermediate values of the resistivity, the reconnection is bistable. We map the hysteresis curve and demonstrate that the transition from slow to fast reconnection is catastrophic. We present a scaling analysis for the resistivities at which transitions occur and propose that the transition is a possible mechanism for reconnection onset in physical systems.

PACS numbers: 52.35.Vd, 52.65.-y

Magnetic reconnection is vastly different depending on the collisionality of the system in question. For high collisionality, resistive reconnection is slow and is marked by a long, thin current layer [1, 2], whereas collisionless reconnection is fast and is marked by a short current layer with a wide outflow nozzle [3, 4, 5, 6, 7, 8]. Previous theoretical investigations of magnetic reconnection have concentrated exclusively on one of the two regimes. In this letter, we discuss the transition between the two as the collisionality of the system is varied.

This transition is important for understanding the onset of reconnection in systems where plasma resistivity η is finite, yet transitions to fast reconnection, where resistivity is unlikely to be important, are observed. Examples are reconnection events in laboratory fusion experiments and eruptions in the solar corona.

For a given plasma resistivity, rather general arguments suggest that there are two solutions (fast and slow) to the reconnection problem, *i.e.*, there is bistability. The Sweet-Parker solution [1, 2] governing slow reconnection is valid provided the half width of the current layer δ exceeds the relevant kinetic scale lengths,

$$\frac{\delta}{L} = \sqrt{\frac{\eta c^2}{4\pi c_A L}} > \frac{d_i}{L}, \frac{\rho_s}{L}, \quad (1)$$

where L is the half length of the Sweet-Parker current sheet, $d_i = c/\omega_{pi}$ is the ion inertial length, $\rho_s = v_{th,i}/\Omega_{ci}$ is the ion Larmor radius, $\omega_{pi} = \sqrt{4\pi n e^2/m_i}$ is the ion plasma frequency, $c_A = B/\sqrt{4\pi n m_i}$ is the ion Alfvén speed, $\Omega_{ci} = eB/m_i c$ is the ion cyclotron frequency, $v_{th,i}$ is the ion thermal speed, B and n are the magnetic field and ion density. The magnetic field is to be evaluated immediately upstream of the current layer. The converse condition, that resistivity be sufficiently small to not impact the whistler or kinetic Alfvén dynamics that drive kinetic reconnection [9], yields a different condition on resistivity, which can also be estimated. The whistler dispersion relation is given by $\omega = k^2 d_e^2 \Omega_{ce} - ik^2 \eta c^2 / 4\pi$, where $d_e = c/\omega_{pe}$ is the electron inertial length, $\omega_{pe} = \sqrt{4\pi n e^2/m_e}$ is the electron plasma frequency, and $\Omega_{ce} = eB/m_e c$ is the electron cyclotron frequency. Since both the reactive and dissipative terms scale like k^2 , dissipation can only dominate if it is

sufficiently large enough to do so at all spatial scales. This occurs when the electron-ion collision frequency,

$$\nu_{ei} = \frac{\eta n e^2}{m_e} \gtrsim \Omega_{ce}, \quad (2)$$

a condition which is not typically satisfied in nature. Thus, at intermediate collisionalities where Eq. (1) is satisfied but Eq. (2) is not, there are two reconnection solutions.

The presence of two solutions suggests that the transition between the two states could be catastrophic rather than smooth. In a catastrophic transition between two states, a small change in a control parameter induces a discontinuous jump in the state of the system. Researchers studying solar eruptions [10] and sawtooth crashes [11] have been attempting to develop a catastrophic onset model. The present work, in contrast to these models, suggests that a catastrophic transition from slow to fast reconnection could occur dynamically through a decrease in the resistivity past a critical value at which resistive effects are superseded by non-MHD effects. In another scenario, an external perturbation could compress the current sheet to a width below the relevant kinetic scale. Either mechanism could produce the explosive onset of fast reconnection seen in nature and laboratory experiments.

Before estimating the resistivities at which transitions between slow and fast reconnection occur, let us recall some salient properties of the two disparate regimes of reconnection, namely resistive and collisionless. For pure resistive reconnection [1, 2], the outflow speed v_{out} scales like the upstream ion Alfvén speed, c_A . Conservation of mass forces $\delta/L \sim v_{in}/v_{out}$, where v_{in} is the inflow speed. The inflow speed is estimated by balancing the diffusion of the magnetic field across the sheet, $\eta c^2 / 4\pi \delta^2$, with convection across the sheet, v_{in}/δ , which yields Eq. (1) with $v_{in} \sim c_A \delta / L$. Simulations have demonstrated that the length L of the current layer is macroscopic [12, 13, 14]. The reconnection electric field $E \sim v_{in} B / c$, which is the rate at which flux reconnects, is proportional to v_{in} . For physical systems of interest, the resistivity is exceedingly small, so the reconnection rate is small, implying that resistive reconnection is slow.

Non-MHD Hall effects greatly enhance the rate of reconnection. In a two-fluid model with electron inertia breaking the frozen-in condition, the ions decouple from the electrons at the ion inertial length scale d_i . The electrons become demagnetized at the electron inertial length scale d_e . The outflow is driven by the whistler wave and $v_{out,e} \sim c_{Ae} = B/\sqrt{4\pi nm_e}$, which is the electron Alfvén velocity evaluated immediately upstream of the electron current sheet (as opposed to the ion current sheet) [15]. It was found in a series of numerical simulations [4] that the inflow speed is on the order of $v_{in,e} \sim 0.1c_{Ae}$ independent of system parameters, corresponding to an electron current sheet with a length $L_e \sim 10d_e$. Thus, since $E \propto v_{in}$, Hall-mediated reconnection is fast and is marked by a relatively short current layer and wide outflow nozzle.

We now present a scaling argument for the resistivities at which transitions between these two reconnection configurations occur. First, consider the influence of the Hall effect on Sweet-Parker reconnection in a slow-to-fast transition. When the resistivity falls below a critical value η_{sf} , the width of the Sweet-Parker layer will fall below d_i , invalidating the model. From Eq. (1), this occurs when

$$\eta_{sf} \frac{c^2}{4\pi} \sim \frac{c_A d_i^2}{L}. \quad (3)$$

For example, in the solar corona, $n \sim 10^{10} \text{ cm}^{-3}$, $L \sim 10^9 \text{ cm}$ and $B \sim 100 \text{ G}$ [16], so $\eta_{sf} \sim 10^{-16} \text{ s}$ in cgs units, corresponding to a temperature of $10^2 \text{ eV} \sim 10^6 \text{ K}$.

Second, for the fast-to-slow transition, we explore the magnitude of the resistivity η_{fs} required to disrupt the electron current layer that develops during Hall driven reconnection. As in the Sweet-Parker analysis, we balance resistive diffusion with convection (here, at the electron inertial scale d_e),

$$\eta_{fs} \frac{c^2}{4\pi d_e^2} \sim \frac{v_{in,e}}{d_e} \sim 0.1 \frac{c_{Ae}}{d_e},$$

or

$$\eta_{fs} \frac{c^2}{4\pi} \sim 0.1 c_A d_i, \quad (4)$$

where $c_A d_e = c_A d_i$, with c_A evaluated upstream of the electron current layer. We can alternately write this condition as $\nu_{fs} \sim 0.1\Omega_{ce}$, which is consistent with Eq. (2). The factor 0.1 in Eq. (4) yields the quantitatively correct transition condition. This value of ν_{fs} is independent of system size and is enormous for most physical systems. Equation (4) suggests that once fast reconnection onsets, resistive effects are unlikely to influence the dynamics.

The results in Eq. (3) and (4) suggest that the region of bistability spans an enormous range of resistivity, namely

$$\frac{\eta_{sf}}{\eta_{fs}} \sim 10 \frac{d_i}{L} \ll 1 \quad (5)$$

because $d_i \ll L$ for most systems of physical interest. For example, the ratio in Eq. (5) is 10^{-6} for the solar corona

data presented earlier. Thus, transitions from fast to slow reconnection occur at much higher resistivities than the reverse, so there are two solutions to the reconnection problem for a large range of resistivity.

These theoretical predictions are tested with numerical simulations using the two-fluid code, f3d, a massively parallel code described elsewhere [17]. For simplicity, we treat an isothermal plasma. The simulations are two dimensional with a slab geometry, of length L_x in the x direction and L_y in the y direction. The initial equilibrium is two Harris sheets, $\mathbf{B} = \hat{\mathbf{x}}B_0 \tanh[(y \pm L_y/4)/w_0]$ with $w_0 = 2d_i$, configured in a double tearing mode configuration with periodic boundary conditions in all directions. The ions are initially stationary and initial pressure balance is enforced by a non-uniform density. A perturbation is imposed on the equilibrium magnetic field of the form $\tilde{\mathbf{B}} = -0.004B_0\hat{\mathbf{z}} \times \nabla(\sin(2\pi x/L_x)(1 + \cos(4\pi(y \pm L_y/4)/L_y)))$. The resistivity η is constant and uniform. We use small fourth-order dissipation to damp waves at the grid scale. The Hall, electron inertia, and resistive terms can be enabled and disabled at will. For these simulations, when the Hall effect is enabled, the electron inertia term is also enabled.

The computational domain must be chosen large enough to have a sizable separation of scales between the resistive and Hall-mediated reconnection rates, but with resolution high enough to resolve the electron inertial scales. We find that a computational domain of $L_x \times L_y = 409.6d_i \times 204.8d_i$, with a resolution of $\Delta x = \Delta y = 0.1d_i$ and an electron to ion mass ratio of $m_e = m_i/25$ (i.e., $d_e = 0.2d_i$), is sufficient. Larger systems would produce greater separations of η_{sf} and η_{fs} but are more computationally challenging.

For this computational domain, we can estimate the critical resistivities η_{sf} and η_{fs} . In evaluating Eq. (3), we take the steady state (Sweet-Parker) total current sheet length $2L$ to be $L_x/2$ (i.e., $L \sim 102.4d_i$) because the dominant unstable mode is the longest wavelength mode. Then, normalizing lengths to d_i and velocities to $c_{A0} = B_0/\sqrt{4\pi n_0 m_i}$, where n_0 is the initial density far from the sheet, we obtain

$$\eta'_{sf} \equiv \eta_{sf} \frac{c^2}{4\pi c_{A0} d_i} \sim \frac{d_i}{L} \sim 0.01.$$

To evaluate Eq. (4), we use the value of $B \sim 0.3B_0$ upstream of the electron current layer measured in the simulations to evaluate c_A , so

$$\eta'_{fs} \equiv \eta_{fs} \frac{c^2}{4\pi c_{A0} d_i} \sim 0.03.$$

For the first set of numerical simulations, we take $\eta' = 0.015$, which lies in the range where both fast and slow solutions are predicted to be valid.

To demonstrate bistability, we perform two related sets of simulations. First, we run a collisionless, Hall-MHD simulation from $t = 0$ until most of the flux has reconnected ($t = 589.5\Omega_{ci}^{-1}$). The normalized reconnection

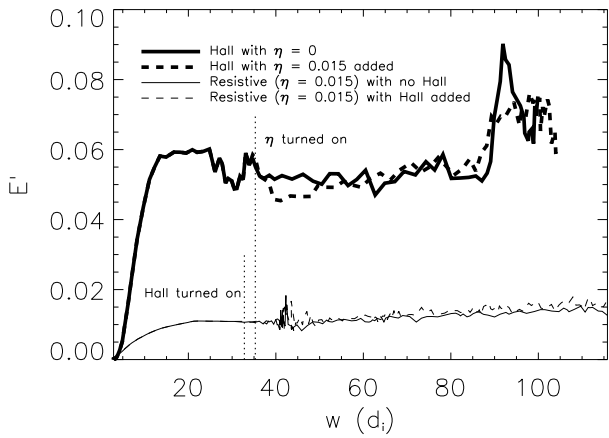


FIG. 1: Normalized reconnection rate, E' , as a function of island width, w , for the two sets of simulations described in the text. The vertical dotted lines show when the added effects were enabled. Note that the parameters of the two dashed simulations are identical.

rate $E' = cE/B_0c_{A0}$ is shown as a function of island width w in the thick solid line in Fig. 1. The reconnection rate is calculated as the time rate of change of magnetic flux between the X-line and O-line. The data has been smoothed with a fourth order algorithm. The rate of reconnection remains nearly constant with $E' \sim 0.06$ beyond an island width of $10d_i$. To explore the impact of collisions, we enable a resistivity of $\eta' = 0.015$ when fast reconnection is already well established ($w \sim 35d_i, t = 409.5\Omega_{ci}^{-1}$) and continue the run (until $t = 648\Omega_{ci}^{-1}$). The result, shown in the thick dashed line in Fig. 1, differs little from the $\eta' = 0$ run.

In the second set of simulations, we run a pure resistive simulation from $t = 0$ with $\eta' = 0.015$ (*i.e.*, the same resistivity) until the magnetic island is large ($t = 2428\Omega_{ci}^{-1}$). The rate of reconnection, shown as the thin solid line in Fig. 1, stabilizes with $E' \sim 0.01$, a full factor of six slower than the fast case. At an island width $w \sim 32d_i$ (at $t = 648\Omega_{ci}^{-1}$), we add the Hall term and run the simulation to late time ($t = 2598\Omega_{ci}^{-1}$). The thin dashed line in Fig. 1 shows that, even after the introduction of the Hall term, the reconnection stays quite near the slow rate of 0.01.

The out of plane current density, J_z , is shown in Fig. 2 at late times for the runs corresponding to the two dashed curves in Fig. 1 (for which both have the same parameters). In the top plot (fast reconnection), the current sheet is short and opens wide, as is expected in Hall-mediated reconnection. In the bottom plot (slow reconnection), the current sheet is long and thin as in Sweet-Parker theory. Since the same equations govern the two sets of data, we conclude that there is bistability, and hence, hysteresis.

Finally, we map the hysteresis curve by finding the steady state reconnection rate, E' , for values of resistivity

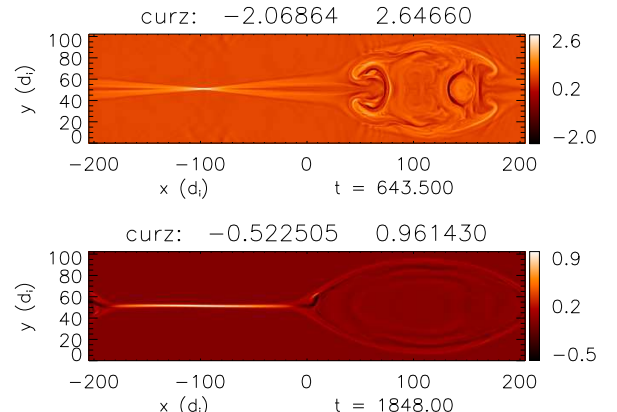


FIG. 2: (Color online) Out of plane current density, J_z , for late times from the two dashed lines of Fig. 1. The top plot corresponds to the heavy dashed line (fast reconnection). The bottom plot corresponds to the thin dashed line (slow reconnection). For simplicity, only one of the two simulated current sheets for each run is shown.

other than 0.015 for both of the previous configurations. For the fast branch, we repeat the runs adding a non-zero resistivity to Hall reconnection (at $t = 409.5\Omega_{ci}^{-1}$), but instead use values of η' of 0.010, 0.020, 0.025 and 0.030. For the slow branch, rather than starting from $t = 0$ with different resistivities, we simply change the resistivity (when $w \sim 50d_i$ at $t = 1098\Omega_{ci}^{-1}$) for the slow reconnection run with $\eta' = 0.015$ and the Hall effect already introduced. We use resistivities of $\eta' = 0.003, 0.007, 0.011, 0.013, 0.020, 0.025$ and 0.030 and evolve the system until it reaches a new steady state. The steady state reconnection rate, E' , is computed as the average reconnection rate over time once transients have died away.

The results are plotted in Fig. 3(a), with the fast branch plotted as open circles and the slow branch plotted as closed circles. The closed circles reveal that the transition from slow to fast reconnection occurs abruptly between η' of 0.011 and 0.013. The open circles reveal a (not so abrupt) transition from fast to slow between η' of 0.020 and 0.025. The error bars are due to the random fluctuations in the steady state reconnection rate. Thus, we see a region of bistability, as expected, and the simulation results show excellent agreement with the scaling law predictions of $\eta'_{fs} \sim 0.01$ and $\eta'_{fs} \sim 0.03$. Fig. 3(b) shows the current sheet width, δ , defined as the half width at half maximum of $J_z(y)$ at the X-line, for each of the above runs. As predicted by the scaling argument, the Sweet-Parker current sheet width, δ , is of order d_i when the transition to fast reconnection occurs, as is shown by the closed circles. Note, the largest resistivity points on the fast branch, at $\eta' = 0.025$ and 0.030, do not relax to the same Sweet-Parker configuration as in the slow branch because, for early times, they are run with zero resistivity while the slow branch contains a non-zero resistivity, so that some flux is dissipated away on the slow branch. Therefore, the configurations are not identical.

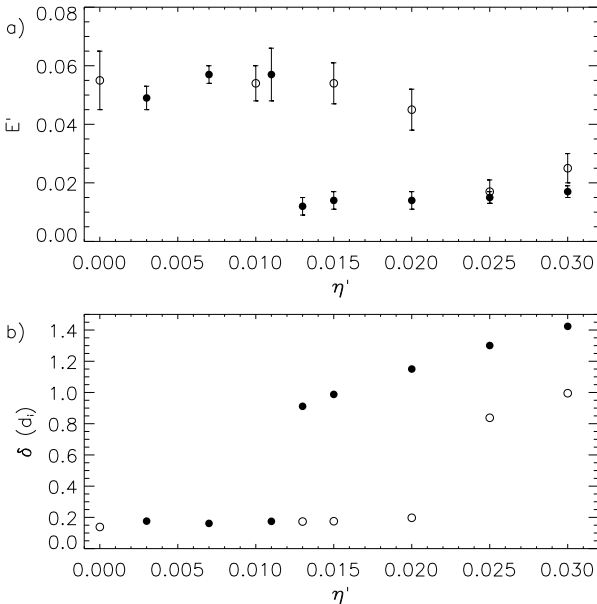


FIG. 3: (a) Steady state normalized reconnection rate, E' , as a function of normalized resistivity, η' for runs analogous to those in Fig. 1 as described in the text. (b) Current sheet width, δ , as a function of η' for the simulations in (a).

The present simulations have been done without a guide field. It is expected that Eq. (3) can be carried over to the guide field case by using ρ_s as the kinetic length scale instead of d_i . This would make it applicable to the sawtooth crash problem in fusion devices. Typical parameters for sawteeth in the DIII-D tokamak [18] are $B_\varphi \sim 2$ T, $T_e \sim 2.0$ keV, $r_s \sim 20$ cm, $n \sim 10^{14}$ cm $^{-3}$ and $Z_{\text{eff}} \sim 2$, and $L \sim r_s \theta$, where $\theta \sim 60^\circ$ is the angular extent of the current layer [11]. For bean-shaped flux

surfaces, the helical field strength in the plasma core is around $B \sim 100$ G, so using Eq. (3) with ρ_s in place of d_i yields $\eta_{sf} \sim 10^{-16}$ s, corresponding to $T \sim 2 \times 10^2$ eV. An extension of the present calculation to include diamagnetic drifts [19] may improve agreement.

The effect of collisionality on the reconnection rate was explored in the Magnetic Reconnection Experiment (MRX) [20]. A sharp increase in the reconnection rate was observed at low collisionality. Data for the current sheet width are unavailable, so further comparisons are not possible.

To summarize, we have demonstrated that both resistive and Hall-mediated reconnection solutions exist simultaneously over a significant range of resistivity. For values of resistivity such that the Sweet-Parker current sheet width is greater than the relevant kinetic length scale (d_i or ρ_s) but does not destroy the electron current sheet, either mechanism can dominate reconnection, depending on the history of the system. A corollary to this result is that if a system is undergoing slow resistive reconnection, a decrease in the resistivity below the critical resistivity is accompanied by an abrupt transition to fast reconnection. Alternately, a large perturbation which reduces the current sheet width of a Sweet-Parker current sheet below the appropriate kinetic scale would presumably also induce a transition to fast reconnection. These scenarios present possible mechanisms for the explosive onset of magnetic reconnection in physical systems. An estimate of the critical temperature in the solar corona agrees rather well with the coronal temperature, but a similar estimate for the sawtooth crash is too small.

This work has been supported by NSF Grant No. PHY-0316197 and DOE Grant Nos. ER54197 and ER54784. Computations were carried out at the National Energy Research Scientific Computing Center.

[1] E. N. Parker, *J. Geophys. Res.* **62**, 509 (1957).
[2] P. A. Sweet, in *Electromagnetic Phenomena in Cosmical Physics*, edited by B. Lehnert (Cambridge University Press, New York, 1958), p. 123.
[3] R. Horiuchi and T. Sato, *Phys. Plasmas* **4**, 277 (1997).
[4] M. A. Shay, J. F. Drake, B. N. Rogers, and R. E. Denton, *Geophys. Res. Lett.* **26**, 2163 (1999).
[5] M. Hesse, J. Birn, and M. Kuznetsova, *J. Geophys. Res.* **106**, 3721 (2001).
[6] M. M. Kuznetsova, M. Hesse, and D. Winske, *J. Geophys. Res.* **106**, 3799 (2001).
[7] P. L. Pritchett, *J. Geophys. Res.* **106**, 3783 (2001).
[8] F. Porcelli, D. Borgogno, F. Califano, D. Grasso, M. Ottaviani, and F. Pegoraro, *Plasma Phys. Control. Fusion* **44**, B389 (2002).
[9] B. N. Rogers, R. E. Denton, J. F. Drake, and M. A. Shay, *Phys. Rev. Lett.* **87**, 195004 (2001).
[10] J. Lin, W. Soon, and S. L. Baliunas, *New Astron. Rev.* **47**, 53 (2003).
[11] L. Zakharov, B. Rogers, and S. Migliuolo, *Phys. Fluids* **5**, 2498 (1993).
[12] D. Biskamp, *Phys. Fluids* **29**, 1520 (1986).
[13] D. A. Uzdensky and R. M. Kulsrud, *Phys. Plasmas* **7**, 4018 (2000).
[14] B. D. Jemella, J. F. Drake, and M. A. Shay, *Phys. Plasmas* **11**, 5668 (2004).
[15] M. A. Shay, J. F. Drake, B. N. Rogers, and R. E. Denton, *J. Geophys. Res.* **106**, 3751 (2001).
[16] J. A. Miller, P. J. Cargill, A. G. Emslie, G. D. Holman, B. R. Dennis, T. N. LaRosa, R. M. Winglee, S. G. Benka, and S. Tsuneta, *J. Geophys. Res.* **102**, 14631 (1997).
[17] M. A. Shay, J. F. Drake, M. Swisdak, and B. N. Rogers, *Phys. Plasmas* **11**, 2199 (2004).
[18] E. A. Lazarus (2005), private communication.
[19] F. M. Levinton, L. Zakharov, S. H. Batha, J. Manickam, and M. C. Zarnstorff, *Phys. Rev. Lett.* **72**, 2895 (1994).
[20] F. Trintchouk, M. Yamada, H. Ji, R. M. Kulsrud, and T. A. Carter, *Phys. Plasmas* **10**, 319 (2003).